Real-time Prognostics of a Rotary Valve Actuator

Matthew Daigle

NASA Ames Research Center, Moffett Field, CA, 94035, USA
matthew.j.daigle@nasa.gov

ABSTRACT

Valves are used in many domains and often have system-critical functions. As such, it is important to monitor the health of valves and their actuators and predict remaining useful life. In this work, we develop a model-based prognostics approach for a rotary valve actuator. Due to limited observability of the component with multiple failure modes, a lumped damage approach is proposed for estimation and prediction of damage progression. In order to support the goal of real-time prognostics, an approach to prediction is developed that does not require online simulation to compute remaining life, rather, a function mapping the damage state to remaining useful life is found offline so that predictions can be made quickly online with a single function evaluation. Simulation results demonstrate the overall methodology, validating the lumped damage approach and demonstrating real-time prognostics.

1. INTRODUCTION

Prognostics is a key technology in the area of systems health management. Failure prognostics specifically deals with the prediction of damage progression, end of useful life (EOL), and remaining useful life (RUL) of a component. Based on these predictions, maintenace can be optimized (Tian, Jin, Wu, & Ding, 2011; Camci, 2009) and/or loads can be reallocated to slow damage progression (Bole et al., 2010; Graham, Dixon, Hubbard, & Harrington, 2014). In cryogenic propellant loading systems (Barber, Johnston, & Daigle, 2013; Zeitlin, Clements, Schaefer, Fawcett, & Brown, 2013), most hardware faults are observed in the valves controlling the flow of propellant (Daigle & Goebel, 2011a), therefore, valve prognostics is a critical technology for safe and efficient cryogenic loading operations. Valve prognostics is critical in many other application domains as well.

Previous work in valve prognostics has focused on pneumatically-actuated valves (Daigle, Kulkarni, & Gorospe, 2014; Tao, Zhao, Zio, Li, & Sun, 2014), where the major fault mode is leaks of the pneumatic gas. As leaks grow over time, a significant performance degradation, as measured by valve opening and closing times, can be observed. Our previous work (Daigle et al., 2014; Kulkarni, Daigle, Gorospe, & Goebel, 2014, 2015) developed a model-based prognostics approach for pneumatic valves based on observation of these features.

In this paper, we investigate prognostics of motor-actuated valves, specifically, rotary-actuator quarter-turn valves. In these valves, there is no pneumatic system, and all actuation is electrical-based. Therefore, other damage modes will dominate, such as an increase in friction (Daigle & Goebel, 2011a) and electrical resistance over the life of the component. Further, while the valves in previous work were operated in a discrete open/close fashion, the valves considered here are actuated in a continuous fashion. In particular, they are used in a replenish operation of cryogenic loading, and so are controlled continuously to, in turn, control the flow of propellant in the vehicle tank to replace any propellant that has boiled off while waiting for launch. Thus, the usage of the valve is much more stochastic, and this presents additional challenges to the prognostics problem.

Here, we develop a model-based prognostics approach for rotary valve actuators in this usage context. In our application, only valve position is measured, and we find that friction and resistance faults cannot, as a result, be distinguished. So, a novel lumped-damage model (a concept familiar in structural mechanics (Marante & Flórez-López, 2003)) is used for damage estimation and failure prediction. We develop also new approaches for dealing with the future component usage in this kind of usage context. Further, our goals are for real-time prognostics, i.e., EOL/RUL predictions must be provided in real-time. To this end, we develop also an efficient model-based prediction based on offline model analysis, finding the functional mapping between valve state and RUL, thus avoiding the need for a computationally costly simulation. Although the goal here is to develop an efficient prognostics solution for the particular valve actuator under study, some of the methods developed in this paper can be applied on a more general level.

Matthew Daigle et al. This is an open-access article distributed under the terms of the Creative Commons Attribution 3.0 United States License, which permits unrestricted use, distribution, and reproduction in any medium, provided the original author and source are credited.

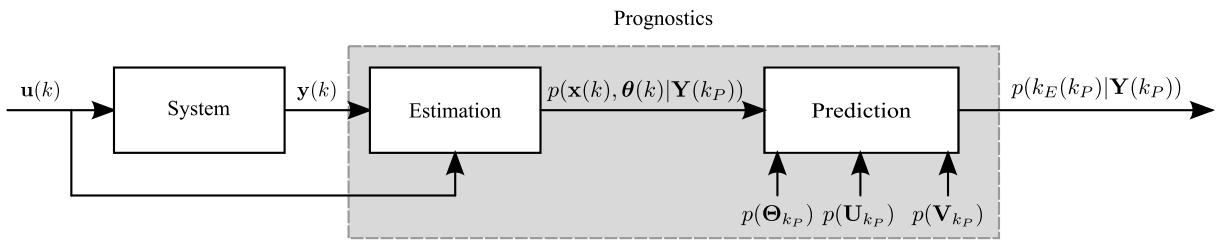

Figure 1. Model-based prognostics architecture.

The paper is organized as follows. Section 2 formulates the prognostics problem and overviews the model-based prognostics approach followed in this paper. Section 3 presents the model of the rotary valve actuator. Section 4 describes the estimation approach, and Section 5 describes the prediction approach. Section 6 demonstrates the overall prognostics approach and presents some experimental results in simulation for validation. Section 7 concludes the paper.

2. MODEL-BASED PROGNOSTICS

In this section, we formulate the prognostics problem, using the framework presented in (Daigle, Sankararaman, & Kulkarni, 2015), which extends the concepts originally presented in (Orchard & Vachtsevanos, 2009; Daigle & Goebel, 2013; Saha & Goebel, 2009). We then provide a computational architecture for model-based prognostics that will be applied to the rotary valve actuator.

2.1. Problem Formulation

We assume the system model may be generally defined as

$$\mathbf{x}(k+1) = \mathbf{f}(k, \mathbf{x}(k), \boldsymbol{\theta}(k), \mathbf{u}(k), \mathbf{v}(k)), \tag{1}$$

$$\mathbf{y}(k) = \mathbf{h}(k, \mathbf{x}(k), \boldsymbol{\theta}(k), \mathbf{u}(k), \mathbf{n}(k)), \tag{2}$$

where k is the discrete time variable, $\mathbf{x}(k) \in \mathbb{R}^{n_x}$ is the state vector, $\boldsymbol{\theta}(k) \in \mathbb{R}^{n_\theta}$ is the unknown parameter vector, $\mathbf{u}(k) \in \mathbb{R}^{n_u}$ is the input vector, $\mathbf{v}(k) \in \mathbb{R}^{n_v}$ is the process noise vector, $\mathbf{f}$ is the state equation, $\mathbf{y}(k) \in \mathbb{R}^{n_y}$ is the output vector, $\mathbf{n}(k) \in \mathbb{R}^{n_n}$ is the measurement noise vector, and $\mathbf{h}$ is the output equation.[1] The unknown parameter vector $\boldsymbol{\theta}(k)$ is used to capture explicit model parameters whose values are unknown and time-varying stochastically.

Prognostics is concerned with predicting the occurrence of some event E that is defined with respect to the states, parameters, and inputs of the system. We define the event as the earliest instant that some event threshold $T_E : \mathbb{R}^{n_x} \times \mathbb{R}^{n_\theta} \times \mathbb{R}^{n_u} \to \mathbb{B}$, where $\mathbb{B} \triangleq \{0, 1\}$, changes from the value 0 to 1. That is, the time of the event k_E at some time of prediction k_P is defined as

$$k_E(k_P) \triangleq \inf\{k \in \mathbb{N} \colon k \geq k_P \wedge T_E(\mathbf{x}(k), \boldsymbol{\theta}(k), \mathbf{u}(k)) = 1\}. \tag{3}$$

The time remaining until that event, Δk_E, is defined as

$$\Delta k_E(k_P) \triangleq k_E(k_P) - k_P. \tag{4}$$

In this paper, E specifically represents the end-of-life event. So, k_E is EOL and Δk_E is RUL.

2.2. Prognostics Architecture

We adopt a model-based prognostics architecture (Daigle & Goebel, 2013; Daigle & Sankararaman, 2013), in which there are two sequential problems, (*i*) the *estimation* problem, which requires determining a joint state-parameter estimate $p(\mathbf{x}(k), \boldsymbol{\theta}(k)|\mathbf{Y}(k_P))$ based on the history of observations up to time k, $\mathbf{Y}(k_P) = [\mathbf{y}(k_0) \ldots \mathbf{y}(k_P)]$, and (*ii*) the *prediction* problem, which determines at k_P, using the joint state-parameter estimate $p(\mathbf{x}(k), \boldsymbol{\theta}(k)|\mathbf{Y}(k_0{:}k_P))$, the future parameter trajectory $p(\boldsymbol{\Theta}_{k_P})$, the future input trajectory $p(\mathbf{U}_{k_P})$, and the future process noise trajectory $p(\mathbf{V}_{k_P})$, a probability distribution $p(k_E(k_P)|\mathbf{Y}(k_P))$.

The prognostics architecture is shown in Fig. 1. In discrete time k, the system is provided with inputs $\mathbf{u}_k$ and provides measured outputs $\mathbf{y}_k$. The estimation module uses this information, along with the system model, to compute an estimate $p(\mathbf{x}(k), \boldsymbol{\theta}(k)|\mathbf{Y}(k))$. The prediction module uses the joint state-parameter distribution and the system model, along with the distributions $p(\boldsymbol{\Theta}_{k_P})$, $p(\mathbf{U}_{k_P})$, and $p(\mathbf{V}_{k_P})$, to compute the probability distribution $p(k_E(k_P)|\mathbf{Y}(k_P))$. We describe an approach to solve the estimation problem in Section 4, and an approach for the prediction problem in Section 5.

3. VALVE MODELING

We consider here a rotary valve actuator (Flowserve Series 75 Actuator) controlled by a digital positioner (Flowserve DFP17). The actuator consists of a DC electric motor, and moves between 0 and 90°, i.e., it is for a quarter-turn valve. A 4–20 mA input signal is provided to command to a desired position, and the positioner outputs ±24 V to rotate the

[1] Bold typeface denotes vectors, and n_a denotes the length of a vector $\mathbf{a}$.

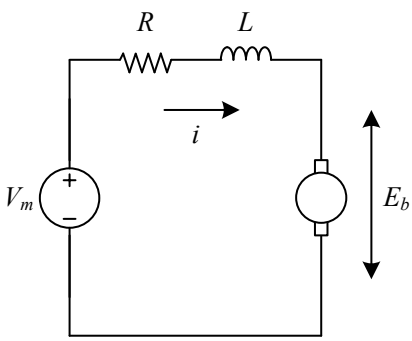

Figure 2. DC motor circuit.

actuator in either direction to meet the position setpoint. A positioner deadband ensures that the commanded voltage is zero when the position error is close enough to the setpoint in order to prevent oscillations around the setpoint.

We develop a physics-based model of the valve actuator. We start by developing the nominal model, and then extend it to include damage modeling.

3.1. Nominal Model

The state variables include the actuator position, θ, and the actuator velocity, ω:

$$\dot{\theta} = \omega, \tag{5}$$
$$\dot{\omega} = \alpha, \tag{6}$$

where α is the angular acceleration, which is based on the torques on the actuator. The torques include the motor torque, τ_m, and the friction torque, τ_f:

$$\alpha = \frac{1}{J}\left(\tau_m - \tau_f\right), \tag{7}$$

where J is the rotational inertia. The torques are defined by

$$\tau_m = Ki, \tag{8}$$
$$\tau_f = b\omega, \tag{9}$$

where K is the motor constant, i is the motor current, and b is the friction coefficient.

The DC motor circuit is shown in Fig. 2. Ignoring the (fast) transients in the motor current (i.e, assuming steady-state for the inductance L, in which the voltage drop is zero), it can be expressed as an algebraic function of the motor voltage V_m and back electromotive force (emf) E_b:

$$i = \frac{V_m - E_b}{R}, \tag{10}$$

where R is the motor electrical resistance. The back emf is described by:

$$E_b = K\omega. \tag{11}$$

The motor voltage is controlled by a positioner. A 4–20 mA input signal, mapping to an angular position between 0 and $\pi/2$, is provided. If the motor position needs to increase, then a positive voltage is provided by the positioner to the motor, and if it needs to decrease, a negative voltage is provided. If the position error is within a small deadband, then zero voltage is given. The positioner is described by the following set of equations:

$$\theta_d = \left(\frac{u-4}{16}\right)\frac{\pi}{2}, \tag{12}$$
$$e_\theta = \theta_d - \theta, \tag{13}$$

where θ_d is the desired position, u is the input signal (in mA), and e_θ is the position error. The voltage is then determined using:

$$V_m = \begin{cases} V_u, & \text{if } |e_\theta| > db \text{ and } e_\theta > 0, \\ -V_u, & \text{if } |e_\theta| > db \text{ and } e_\theta < 0, \\ 0, & \text{otherwise.} \end{cases} \tag{14}$$

where V_u is the input voltage, and db is the deadband.

Here, only one sensor is available, which is the position:

$$\theta^* = \theta\frac{180}{\pi}, \tag{15}$$

where θ^* is the measured position in degrees.

In summary:

$$\mathbf{x}(t) = [\theta(t)\ \omega(t)]^T,$$
$$\mathbf{u}(t) = [u(t)],$$
$$\mathbf{y}(t) = [\theta^*(t)].$$

3.2. Damage Modeling

Based on discussion with subject matter experts, we consider two distinct damage modes, an increase in internal friction (as captured by the friction coefficient b) and an increase in internal electrical resistance (R). We assume that the friction coefficient increases as a function of an unknown wear parameter, w_b, the motor speed, ω, and the friction force, $b \cdot \omega$, as described in (Daigle & Goebel, 2013):

$$\dot{b} = w_b \cdot b \cdot \omega^2, \tag{16}$$

which is based on the basic wear equation (Hutchings, 1992). Note that friction damage only progresses when the valve is in motion.

Similarly, we assume that electrical resistance increases as a function of an unknown wear parameter w_R and the motor electrical power, $V_m i$:

$$\dot{R} = w_R |V_m i|. \tag{17}$$

Note that resistance will only increase when there is power applied to the motor.

In the extended model, we now have:

$$\begin{aligned}
\mathbf{x}(t) &= [\theta(t)\ \omega(t)\ b(t)\ R(t)]^T, \\
\boldsymbol{\theta}(t) &= [w_b\ w_R], \\
\mathbf{u}(t) &= [u(t)], \\
\mathbf{y}(t) &= [\theta^*(t)].
\end{aligned}$$

3.3. End of Life

In past valve prognostics applications, the valves were operated in a discrete open/close fashion, so the EOL threshold could be expressed based on required open/close times (Daigle & Goebel, 2011a, 2009). However, in this case, the valve position is controlled continuously, so the valve may never even go through an open/close cycle in actual operation. Thus, the EOL definition must be generalized.

Instead, we can measure degradation through the steady-state valve velocity, ω_{ss}, which is fundamentally equivalent to using open/close time thresholds. A major difference, however, is that ω_{ss} cannot be directly measured.

In the steady state, $\dot{\omega} = 0$, and so angular acceleration is zero and the motor and friction torques must balance, i.e., $\tau_m = \tau_f$ (by Eq. 7). Assuming $w_{ss} > 0$, i.e., $V_m = V_u$, this means that (using substitutions from Eqs. 8, 9, 10 and 11):

$$\begin{aligned}
Ki &= b\omega_{ss}, \\
K\left(\frac{V_u - E_b}{R}\right) &= b\omega_{ss}, \\
K\left(\frac{V_u - K\omega_{ss}}{R}\right) &= b\omega_{ss},
\end{aligned}$$

and, so, solving for ω_{ss}, we have

$$\omega_{ss} = \frac{V_u K}{K^2 + bR}. \tag{18}$$

Now, we express EOL using a minimum steady-state velocity value, ω_{ss}^-:

$$T_E = \omega_{ss} \leq \omega_{ss}^-, \tag{19}$$

i.e., E (EOL) is reached when the steady-state velocity reaches its minimum value. Since ω_{ss} is a function of the damage variables b and R, given estimates of these variables an estimate of ω_{ss} may be computed for the purposes of EOL prediction.

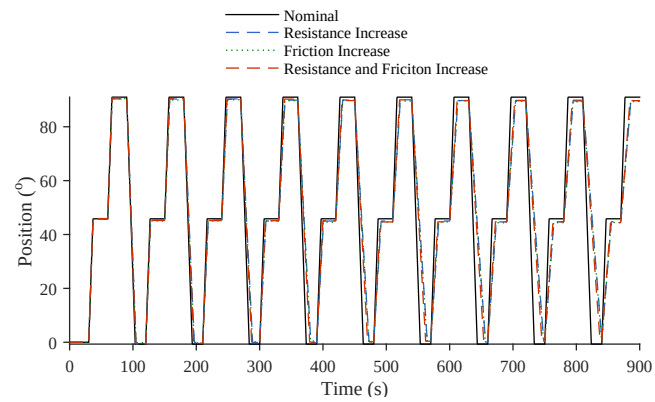

Figure 3. Damage progression with combinations of damage modes.

4. ESTIMATION

The goal of the estimation step is to compute a joint state-parameter estimate based on the measured system outputs. As described in Section 3, here, only position is measured. However, there are two distinct damage modes that may occur. In fact, we cannot distinguish between these two faults based only on the position sensor. As shown in Fig. 3, the two damage progressions look the same. A zero w_R and nonzero w_b can produce observations that look like a nonzero w_R and a zero w_b, as well as a nonzero w_R and nonzero w_b. Even without sensor noise it is difficult to observe any difference, so with sensor noise, it will not be possible to distinguish them.

This lack of distinguishability is implied by the w_{ss} relation. In Eq. 18, both b and R appear in the denominator. For example, if b doubles, w_{ss} will look the same as if R doubles, or the product bR doubles. The damage progressions for b and R are similar enough that as they grow over time one can always be mistaken for the other, and for this reason, it will be very difficult to distinguish one from the other or some combination of effects. Fundamentally, this is an observability problem. We have two damage modes but only one sensor, and the estimation problem is under-constrained. In longer time horizons, Fig. 3 suggests that the ambiguity remains.

Since there is practically no hope in distinguishing the damage mode or combination of damage modes occurring, we can simplify the model and use a lumped damage approach. That is, we can estimate an equivalent single damage and damage progression rate, and make EOL predictions based on the lumped damage estimate. Since any combination of damage progressions looks like a friction damage progression, we just use the valve model minus the constraint describing the growth of the resistance parameter (Eq. 17), remove R from

$\mathbf{x}(t)$, and remove w_R from $\boldsymbol{\theta}(t)$.[2] If we can still make accurate EOL predictions no matter the combination of damage modes, then this approximation is acceptable.

We use the unscented Kalman filter (UKF) (Julier & Uhlmann, 2004) for joint state-parameter estimation for the lumped damage model. Details on the filter can be found in (Julier & Uhlmann, 2004) and its application to prognostics in (Daigle, Saha, & Goebel, 2012). To perform joint state-parameter estimation for the UKF, the state vector is augmented with the parameter vector, i.e, unknown parameters are treated as states. The parameters are assumed to evolve only via process noise terms.

It is well-known that the variance used for the process noise for the unknown parameters should be tuned online for optimal performance, and this has been addressed in the context of UKFs (Daigle et al., 2012; Daigle & Goebel, 2013) and particle filters (Orchard, Tobar, & Vachtsevanos, 2009; Liu & West, 2001; Daigle & Goebel, 2011b). We use here the approach developed in (Daigle & Goebel, 2013), in which a *relative* measure of spread on the unknown parameters (in this case, the wear parameter w_b) is controlled. A large variance is used initially to encourage convergence, and once convergence is reached, a small variance is used. The variance is increased or decreased proportionally to the error in the desired relative spread (e.g., 10%) from the actual spread currently estimated by the UKF. Details of the algorithm and pseudocode can be found in (Daigle & Goebel, 2013). Here, we initially control to a relative spread of 50% (as measured by relative standard deviation of the estimated wear parameter), and once convergence is achieved (determined by the initial relative spread being reached), then we control the relative spread to 15%.

5. PREDICTION

The goal of the prediction step is to, given the joint state-parameter estimate, predict EOL and RUL. However, in order to make a prediction, we require also an understanding of the uncertainty in the inputs to the prediction problem (Sankararaman, Daigle, Saxena, & Goebel, 2013). The inputs to the prediction problem include the state-parameter estimate, the future input trajectory, the future process noise trajectory, and the future parameter trajectory. For the purposes of this paper, we assume that process noise is negligible relative to the future input uncertainty, and that the parameters are constant (although uncertain at the time of prediction).

5.1. Future Input Uncertainty

Consideration of the future input uncertainty is critical to making accurate and useful predictions. Characterizing this uncertainty depends heavily on the application at hand. For the rotary valve actuator, the valve is used in a replenish mode for cryogenic propellant loading, in which the flow through the valve is controlled to replace any boil off in the vehicle tank due to heat exchange with the environment.

There are two important things to note about its usage. First, the valve is used only in a certain mode of operation. Thus, it makes sense only to report EOL/RUL in terms of usage time, not absolute time. This is because (*i*) we do not know how long the replenish operation will take, and (*ii*) we do not know how long the valve will be sitting unused between replenish operations.

Second, the valve can be in use but with no damage progressing. There must be motion of the actuator for the friction damage to increase (by Eq. 16) and current flowing through the actuator motor for the resistance damage to increase (by Eq. 17). If the actuator has reached its position setpoint within the deadband, then motor voltage and current are zero, and the valve is not moving, but the valve is still being used in the sense that it is receiving a command and responding to it. Thus, if we want to make a prediction in terms of usage hours, we must acknowledge the fact that for an (unknown) percentage of the time the valve is being used, it is not moving and damage is not progressing.

Given these considerations, a true future input trajectory will be interspersed with both nonusage time and usage time, and the usage time will be further divided into time in which the actuator is moving and damage is progressing, and time in which the actuator is not moving and damage is not progressing. If we only want a prediction in terms of usage hours, then we do not need to waste time simulating trajectories to EOL including nonusage time. We do not also need to waste time simulating trajectories in which there are intervals in which damage is not progressing; instead, we can predict assuming damage is always progressing, and then correct the predictions using statistical information on the percentage of time the actuator is actually moving.

So, to make an RUL prediction, we need only a subset of the model in which we compute T_E using V_m as an input, in which V_m is always 24 V. In this case, the actuator will continuously move and damage continuously progress. The needed submodel can be derived from the model equations using the general structural model decomposition framework presented in (Roychoudhury, Daigle, Bregon, & Pulido, 2013). Using the `GenerateSubmodel` algorithm in that work, we can compute the minimal subset of model equations needed to compute T_E using V_m. In this case, we find that we require only Eqs. 6–11, 16, 18, and 19.

So, given a sample of the system state, we can simulate until T_E evaluates to 1 and obtain corresponding EOL and RUL predictions. In order to correct these predictions, we require

[2] Since any combination of damage progressions also looks like a resistance damage progression, we could equivalently use that model to represent the lumped damage instead.

Algorithm 1 $k_E(k_P) \leftarrow \mathtt{P}(\mathbf{x}(k_P), \mathbf{\Theta}_{k_P}, \mathbf{U}_{k_P}, \mathbf{V}_{k_P})$

$k \leftarrow k_P$
$\mathbf{x}(k) \leftarrow \mathbf{x}(k_P)$
$\mathbf{z}(k_P) \leftarrow \mathbf{g}(k, \mathbf{x}(k), \mathbf{\Theta}_{k_P}(k), \mathbf{U}_{k_P}(k))$
while $T_E(\mathbf{x}(k), \mathbf{\Theta}_{k_P}(k), \mathbf{U}_{k_P}(k)) = 0$ **do**
  $\mathbf{x}(k+1) \leftarrow \mathbf{f}(k, \mathbf{x}(k), \mathbf{\Theta}_{k_P}(k), \mathbf{U}_{k_P}(k), \mathbf{V}_{k_P}(k))$
  $k \leftarrow k+1$
  $\mathbf{x}(k) \leftarrow \mathbf{x}(k+1)$
end while
$k_E(k_P) \leftarrow k$

statistics on the percentage of the actuator usage in which it is actually moving. We assume that, while being used, the statistics of the past and future behavior in this context are equivalent. Thus, we use the history of past sensor measurements to keep track of when the actuator is moving and when it is not in order to compute these statistics. We have a binary distribution; either the acutator is moving or not. We define f_m as the fraction of the time that the actuator is moving while in usage. The actuator is considered to be moving when the absolute value of the estimated velocity is greater than some threshold (i.e., 0.01 rad/s). Then, f_m is computed as the amount of usage time this condition is satisfied over the total amount of usage time. We then compute the corrected RUL, $\Delta k_{E,f_m}$, based on the predicted RUL assuming full-time movement, $\Delta k_{E,100\%}$, as:

$$\Delta k_{E,f_m} = \frac{\Delta k_{E,100\%}}{f_m}. \tag{20}$$

The corrected EOL can then be computed based on corrected RUL:

$$k_{E,f_m} = \Delta k_{E,f_m} + k_P, \tag{21}$$

where k_P is the time of prediction.

5.2. RUL Computation

Given the state estimate, we can sample from its distribution, simulate each sample to E, and obtain corresponding k_E values using Algorithm 1 (Daigle & Sankararaman, 2013). We can then correct these predictions using Eqs. 20 and 21 to obtain the desired EOL/RUL distribution. Recall, however, that we have the requirement of real-time prognostics, that is, we must compute the prediction for time k before time $k+1$. This is a difficult problem, considering that we must perform a simulation to E, and the amount of time the simulation takes depends on the rate of damage progression, which, in reality, is very small.

A solution to this problem is to move the simulations from online computation to offline, design-time computation. We may construct a lookup table for this purpose, in which different values of the state are simulated to EOL and the result stored, so that a mapping from states to RUL is established. Lookup tables have been used previously in prognostics in the context of damage estimation (Teubert & Daigle, 2013, 2014; Daigle et al., 2014). However, the problem with a lookup table is that it has only a finite number of elements, so the precision and range of the table is finite. In reality, the wear rates can take a variety of values and it is difficult to capture a suitable domain. The granularity of the table will also determine the precision of the RUL predictions available.

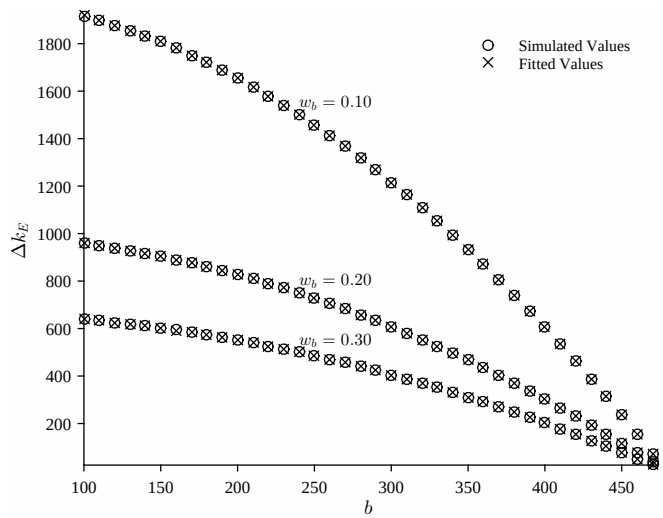

Figure 4. Second-order polynomial fits to Δk_E values compared to simulated Δk_E values as a function of b for different values of w_b.

So, instead of using a lookup table, here, we find the direct functional mapping from the actuator state to RUL, i.e., $\Delta k_E = g(\mathbf{x})$. In the lumped damage approximation, and assuming $f_m = 100\%$, only b and w_b will have an effect on the RUL prediction, so we have to find a function of only two inputs that computes RUL, i.e., $\Delta k_E = g(b, w_b)$. We first simulate to EOL for a range of states, and then use optimization methods to fit a the function g to the values.

To determine the structure of this equation, we first consider only a single value of w_b, so we have RUL as a function of only b. We find that in this case, a second order polynomial fits very well for any given w_b, as shown in Fig. 4:

$$p_{b,0} + p_{b,1} b + p_{b,2} b^2. \tag{22}$$

Now, we need to determine how the p_b parameters change as a function of w_b. We find that these coefficients are propor-

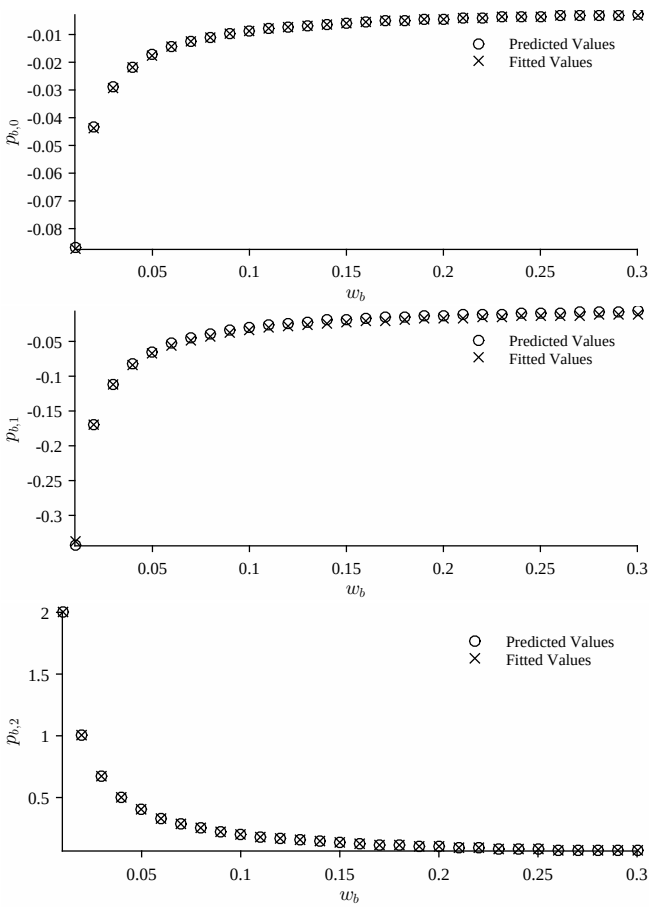

Figure 5. Fitting the polynomial coefficients as a function of w_b.

tional to the inverse of w_b, as shown in Fig. 5:

$$p_{b,0} = \frac{p_0}{w_b}, \tag{23}$$

$$p_{b,1} = \frac{p_1}{w_b}, \tag{24}$$

$$p_{b,2} = \frac{p_2}{w_b}. \tag{25}$$

Now, we have a structure for the overall function:

$$\Delta k_E = \frac{p_0}{w_b} + \frac{p_1}{w_b} b + \frac{p_2}{w_b} b^2. \tag{26}$$

Fig. 6 shows the match between the function values and the simulated values. An excellent fit is obtained.

Summarizing the overall approach, online we estimate the damage state of the acutator using the UKF. We estimate f_m, i.e, how often the actuator is moving while being used. We then map the state estimate distribution to an RUL distribution using Eq. 26. We then correct the RUL distribution using Eq. 20 and the estimated value of f_m. The computation at

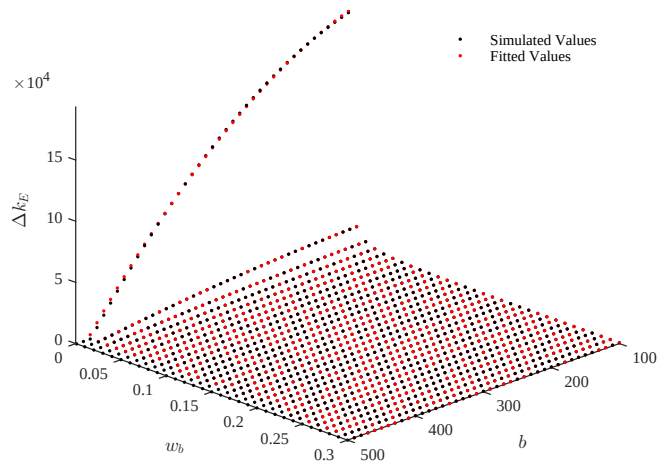

Figure 6. Fitting function Δk_E values compared to simulated Δk_E values.

each step is constant and small relative to the time step, and can be completed in real-time or faster.

6. RESULTS

We validate the overall prognostics approach with a set of simulation-based experiments. Our goals are threefold: (*i*) demonstrate successful estimation of the lumped damage progression, (*ii*) demonstrate accurate prediction with the lumped damage model, and (*iii*) demonstrate accurate prediction with varying levels of component usage. In all scenarios, the valve is always in usage, and so absolute time is equivalent to usage time. Since EOL/RUL are reported in usage time, the true RUL only has the downward slope of -1 when plotted against usage time.

We consider first a scenario in which only friction damage is present, and the desired position is constantly changing, so that the valve is always in motion (i.e., $f_m \approx 100\%$). Fig. 7 shows the lumped damage estimation, and Fig. 8 shows the wear parameter estimate, including the mean, mininimum, and maximum values from the sigma points of the UKF. With the UKF and the properly tuned variance control algorithm, convergence happens relatively quickly, in about 1000 s (roughly 10% of the true k_E). Due to noise and the slow damage progression, the mean deviates, but the resulting predictions are fairly accurate, as shown in Fig. 9. Using a relative accuracy measure of $\alpha = 0.25$, we find that the mean Δk_E prediction falls within the accuracy bounds for most of the time after estimation convergence. In this case, f_m is estimated to be slightly less than 100%, so the corrected predictions are shifted up slightly. This error is due to the noise introduced in the f_m computation as a result of the uncertain estimate of the actuator velocity and the use of the velocity threshold for determining if the valve is moving.

We consider next a similar scenario, except where only resis-

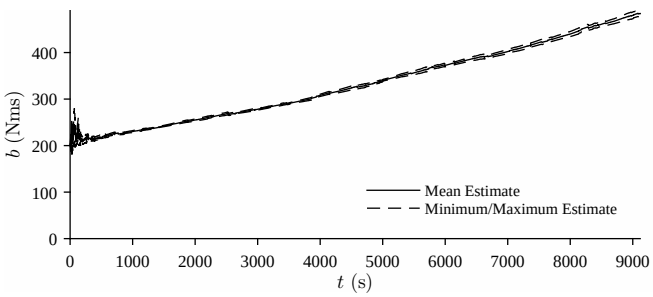

Figure 7. b estimation for $f_m \approx 100\%$ with only friction damage.

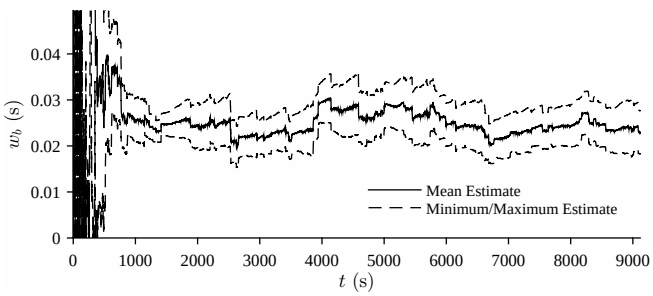

Figure 8. w_b estimation for $f_m \approx 100\%$ with only friction damage.

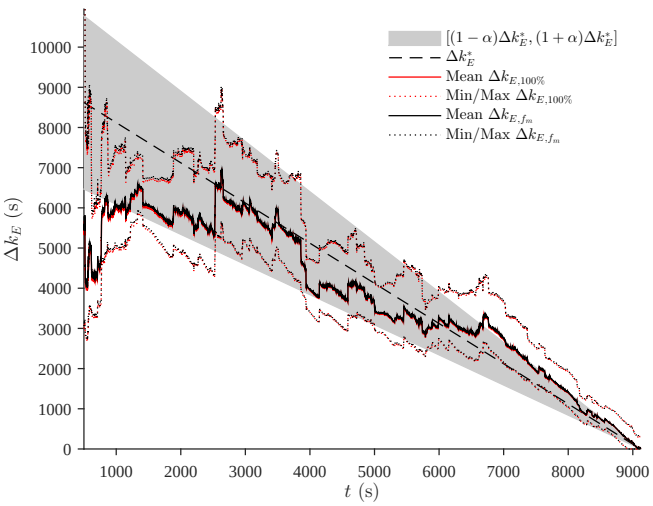

Figure 9. Δk_E predictions for $f_m \approx 100\%$ with only friction damage.

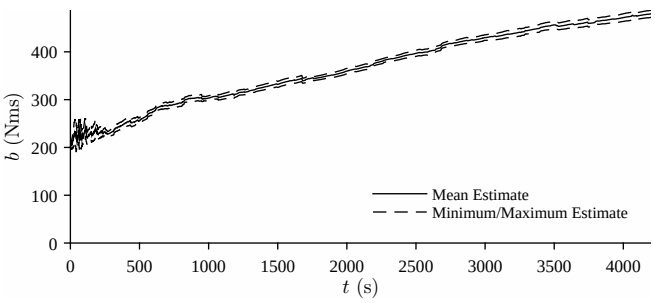

Figure 10. b estimation for $f_m \approx 100\%$ with only resistance damage.

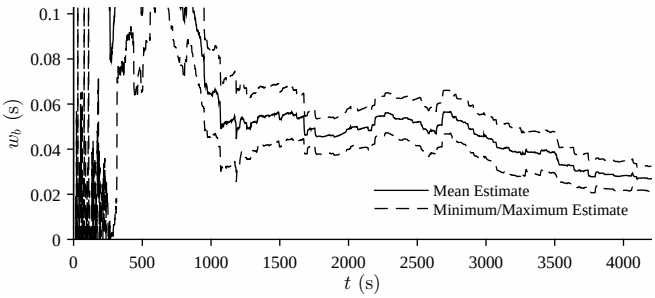

Figure 11. w_b estimation for $f_m \approx 100\%$ with only resistance damage.

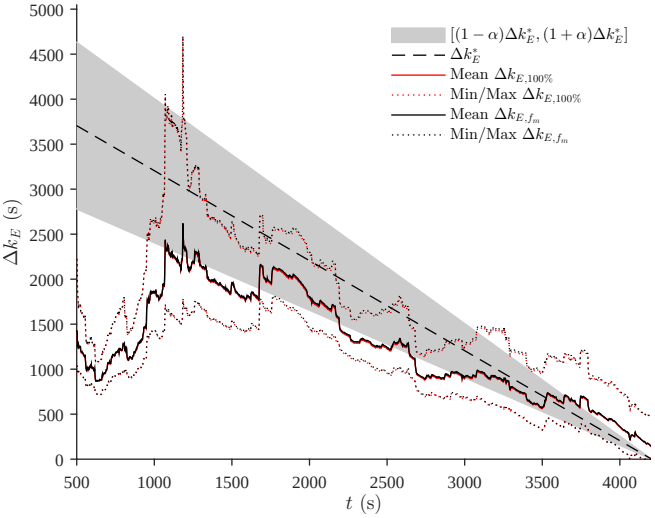

Figure 12. Δk_E predictions for $f_m \approx 100\%$ with only resistance damage.

tance damage is present. Fig. 10 shows the lumped damage estimate, and here it is clear that its shape looks very similar to that when only friction damage is present (Fig. 7). As a result, the wear parameter estimate, shown in Fig. 11, converges, although it is not as steady as the estimate for only friction damage. The predictions, shown in Fig. 12, are fairly accurate once convergence of the wear parameter estimate occurs (which is relatively slower than in the previous scenario).

We consider next a scenario in which both friction and resistance damage modes are progressing, and the component usage is where $f_m \approx 75\%$. Here, the estimation performance is similar to the first scenario, and the wear parameter estimate converges relatively quickly, even though both damage modes are present, i.e, the lumped damage approximation works fairly well. As k_E is approached, the actual future f_m is higher than estimated so the uncorrected predictions be-

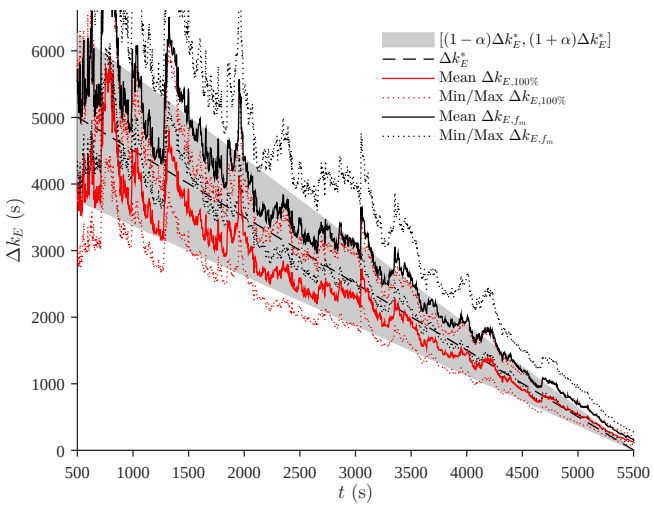

Figure 13. Δk_E predictions for $f_m \approx 75\%$ with combined friction and resistance damage.

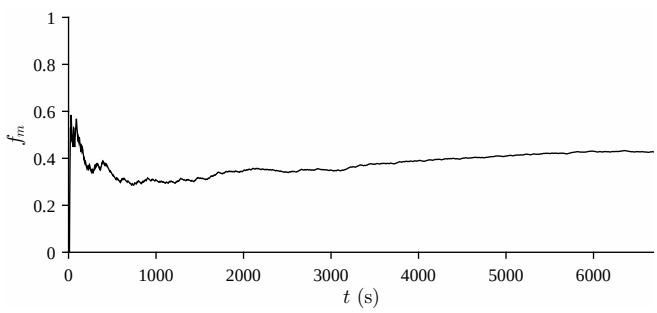

Figure 14. f_m esimate for $f_m \approx 50\%$ with combined friction and resistance damage.

come more accurate, i.e., the assumption that the future value of f_m is the same as the past value is violated, resulting in inaccurate predictions. In practice, some uncertainty should be considered for f_m.

Finally, we consider a similar scenario to the last, except with $f_m \approx 50\%$. Estimation results are similar as in the previous scenario; the wear parameter estimate converges and remains approximately the same once convergence is achieved. The estimate for f_m is shown in Fig. 14, and Δk_E predictions are shown in Fig. 15. It takes some time for the f_m estimate to converge. Early on, f_m is higher than it will be in the future, and so the predictions are overly optimistic, falling outside the accuracy bounds. Convergence occurs at roughly 3500 s, at which point the predictions become much more accurate (here, fluctations are due to those in the wear parameter estimate). After this point, the corrected predictions are much more accurate than the uncorrected ones, which are too pessimistic (overly conservative).

Overall, performance is quite good. Regarding the real-time performance, each second of real time takes only about

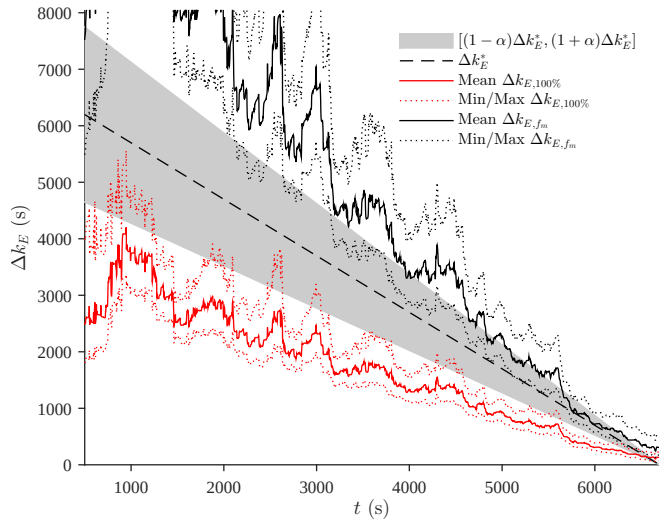

Figure 15. Δk_E predictions for $f_m \approx 50\%$ with combined friction and resistance damage.

0.024 s of processing, which includes both estimation and prediction. Thus, the goal of real-time prognostics is easily achieved, being able to run over 40 times faster than real time.

7. CONCLUSIONS

In this paper, we applied the model-based prognostics approach to a rotary valve actuator. This case study presented several challenges for which new methods were developed to achieve prognostics. First, due to limited observability, a lumped damage approximation was used, which was found to be sufficiently accurate in this case. Note, however, that this will not apply in general; it works here due to the similar effect of the two independent damage modes on the single observable variable. Second, real-time prognostics was a requirement, so instead of online simulation to EOL, offline simulations were performed and an algebraic function was found mapping the damage space to RUL. Thus, for any system state, RUL could be computed extremely quickly, enabling the real-time performance requirement. This approach can be applied to any system, although in some cases it may be difficult to find such a function, especially for high-dimensional damage spaces. Third, we implemented an RUL correction procedure, since predictions were based on 100% movement of the actuator, when in reality during an actual usage, damage only progresses when the valve is moving, which, in our usage context, was stochastic.

In future work, some uncertainty regarding f_m should be considered, as it was not generally true that f_m computed over past values matched f_m computed over future values. Second, accelerated damage progressions (high wear rate values) were considered here for the purposes of demonstration. In reality, wear rates will be much smaller, and this may require

the splitting of dynamics into fast- and slow-time dynamics, with different estimation methods for each (Luo, Pattipati, Qiao, & Chigusa, 2008).

ACKNOWLEDGMENT

This work was supported by the NASA's Advanced Ground Systems Maintenance (AGSM) Project in the Ground Systems Development and Operations (GSDO) Program in the Human Exploration and Operations Mission Directorate.

REFERENCES

Barber, J., Johnston, K., & Daigle, M. (2013, October). A cryogenic fluid system simulation in support of integrated systems health management. In *Annual Conference of the Prognostics and Health Management Society 2013* (p. 114-126).

Bole, B. M., Brown, D. W., Pei, H.-L., Goebel, K., Tang, L., & Vachtsevanos, G. (2010). Load allocation for risk management in overactuated systems experiencing incipient failure conditions. In *2010 Conference on Control and Fault-Tolerant Systems* (pp. 382–386).

Camci, F. (2009). System maintenance scheduling with prognostics information using genetic algorithm. *IEEE Transactions on Reliability*, *58*(3), 539–552.

Daigle, M., & Goebel, K. (2009, September). Model-based prognostics with fixed-lag particle filters. In *Proceedings of the Annual Conference of the Prognostics and Health Management Society 2009.*

Daigle, M., & Goebel, K. (2011a, August). A model-based prognostics approach applied to pneumatic valves. *International Journal of Prognostics and Health Management*, *2*(2).

Daigle, M., & Goebel, K. (2011b, March). Multiple damage progression paths in model-based prognostics. In *Proceedings of the 2011 IEEE Aerospace Conference.*

Daigle, M., & Goebel, K. (2013, May). Model-based prognostics with concurrent damage progression processes. *IEEE Transactions on Systems, Man, and Cybernetics: Systems*, *43*(4), 535-546.

Daigle, M., Kulkarni, C., & Gorospe, G. (2014, March). Application of model-based prognostics to a pneumatic valves testbed. In *Proceedings of the 2014 IEEE Aerospace Conference.*

Daigle, M., Saha, B., & Goebel, K. (2012, March). A comparison of filter-based approaches for model-based prognostics. In *2012 IEEE Aerospace Conference.*

Daigle, M., & Sankararaman, S. (2013, October). Advanced methods for determining prediction uncertainty in model-based prognostics with application to planetary rovers. In *Annual Conference of the Prognostics and Health Management Society 2013* (p. 262-274).

Daigle, M., Sankararaman, S., & Kulkarni, C. (2015, March). Stochastic prediction of remaining driving time and distance for a planetary rover. In *IEEE Aerospace Conference.*

Graham, J. H., Dixon, R., Hubbard, P., & Harrington, I. (2014). *Managing loads on aircraft generators to prevent overheat in-flight* (Tech. Rep. No. 2014-01-2195). SAE.

Hutchings, I. M. (1992). *Tribology: friction and wear of engineering materials*. CRC Press.

Julier, S. J., & Uhlmann, J. K. (2004, Mar). Unscented filtering and nonlinear estimation. *Proceedings of the IEEE*, *92*(3), 401–422.

Kulkarni, C., Daigle, M., Gorospe, G., & Goebel, K. (2014, September). Validation of model-based prognostics for pneumatic valves in a demonstration testbed. In *Annual Conference of the Prognostics and Health Management Society 2014* (p. 76-85).

Kulkarni, C., Daigle, M., Gorospe, G., & Goebel, K. (2015, January). Application of model based prognostics to pneumatic valves in a cryogenic propellant loading testbed. In *AIAA SciTech Conference.*

Liu, J., & West, M. (2001). Combined parameter and state estimation in simulation-based filtering. *Sequential Monte Carlo Methods in Practice*, 197–223.

Luo, J., Pattipati, K. R., Qiao, L., & Chigusa, S. (2008, September). Model-based prognostic techniques applied to a suspension system. *IEEE Transactions on Systems, Man and Cybernetics, Part A: Systems and Humans*, *38*(5), 1156 -1168.

Marante, M. E., & Flórez-López, J. (2003). Three-dimensional analysis of reinforced concrete frames based on lumped damage mechanics. *International Journal of Solids and Structures*, *40*(19), 5109–5123.

Orchard, M., Tobar, F., & Vachtsevanos, G. (2009, December). Outer feedback correction loops in particle filtering-based prognostic algorithms: Statistical performance comparison. *Studies in Informatics and Control*(4), 295-304.

Orchard, M., & Vachtsevanos, G. (2009, June). A particle filtering approach for on-line fault diagnosis and failure prognosis. *Transactions of the Institute of Measurement and Control*(3-4), 221-246.

Roychoudhury, I., Daigle, M., Bregon, A., & Pulido, B. (2013, March). A structural model decomposition framework for systems health management. In *2013 IEEE Aerospace Conference.*

Saha, B., & Goebel, K. (2009, September). Modeling Li-ion battery capacity depletion in a particle filtering framework. In *Proceedings of the Annual Conference of the Prognostics and Health Management Society 2009.*

Sankararaman, S., Daigle, M., Saxena, A., & Goebel, K. (2013, March). Analytical algorithms to quantify the uncertainty in remaining useful life prediction. In *2013 IEEE Aerospace Conference.*

Tao, T., Zhao, W., Zio, E., Li, Y.-F., & Sun, J. (2014).

Condition-based component replacement of the pneumatic valve with the unscented particle filter. In *Prognostics and System Health Management Conference* (pp. 290–296).

Teubert, C., & Daigle, M. (2013, October). I/P transducer application of model-based wear detection and estimation using steady state conditions. In *Annual Conference of the Prognostics and Health Management Society 2013* (p. 134-140).

Teubert, C., & Daigle, M. (2014, March). Current/pressure transducer application of model-based prognostics using steady state conditions. In *2014 IEEE Aerospace Conference.*

Tian, Z., Jin, T., Wu, B., & Ding, F. (2011). Condition based maintenance optimization for wind power generation systems under continuous monitoring. *Renewable Energy*, *36*(5), 1502–1509.

Zeitlin, N. P., Clements, G. R., Schaefer, S. J., Fawcett, M. K., & Brown, B. L. (2013, March). Ground and launch systems processing technologies to reduce overall mission life cycle cost. In *2013 IEEE Aerospace Conference.*